

Theory of the double-edge molecular technique for Doppler lidar wind measurement

Cristina Flesia and C. Laurence Korb

The theory of the double-edge lidar technique for measuring the wind with molecular backscatter is described. Two high-spectral-resolution edge filters are located in the wings of the Rayleigh–Brillouin profile. This doubles the signal change per unit Doppler shift, the sensitivity, and improves measurement accuracy relative to the single-edge technique by nearly a factor of 2. The use of a crossover region where the sensitivity of a molecular- and an aerosol-based measurement is equal is described. Use of this region desensitizes the molecular measurement to the effects of aerosol scattering over a velocity range of ± 100 m/s. We give methods for correcting short-term, shot-to-shot, frequency jitter and drift with a laser reference frequency measurement and methods for long-term frequency correction with a servo control system. The effects of Rayleigh–Brillouin scattering on the measurement are shown to be significant and are included in the analysis. Simulations for a conical scanning satellite-based lidar at 355 nm show an accuracy of 2–3 m/s for altitudes of 2–15 km for a 1-km vertical resolution, a satellite altitude of 400 km, and a 200 km \times 200 km spatial resolution. © 1999 Optical Society of America

OCIS codes: 010.0010, 280.0280, 280.3640, 280.3340, 280.5830.

1. Introduction

Direct-detection lidar techniques for measuring the atmospheric wind field use either aerosol^{1–7} or molecular^{1,8–10} backscatter. The aerosol backscattered spectrum is narrow with respect to the laser width and as a result has the same spectral width as the outgoing laser. Aerosol-based wind measurements thus offer the possibility of high spectral resolution, high sensitivity measurements in those areas where the aerosol backscatter is high. However, large regions of the southern hemisphere as well as mid-oceanic regions have low aerosol concentrations in the free troposphere.¹¹ As a result, current aerosol systems cannot be used for complete global coverage over the troposphere. Alternatively, the molecular backscattered spectrum is broad, which limits the sensitivity of the measurements. However, the molecular scattering provides a dependable and reasonably uniform source of scattering on a

global basis. This is particularly important for making satellite-based wind measurements.

In this paper we describe a double-edge lidar technique for measuring the wind with the molecular signal backscattered from the atmosphere. The method is similar to the single-edge molecular method for determining the wind that was described in 1992 (Ref. 1). In both cases we measure the wind as the average drift velocity of the molecular motion. The molecular signal is spectrally broadened by Doppler shifts that are due to the random thermal motion of molecules, and by Brillouin scattering.^{12–15} With the single-edge method we measure the Doppler shift of this Rayleigh–Brillouin (R-B) spectrum by locating it on a moderately sharp spectral edge of a high-spectral-resolution optical filter. Relatively large changes in measured signal are observed for small frequency shifts that are due to the steep slope of the edge. A small portion of the outgoing beam is sampled to determine the frequency of the outgoing laser signal by measurement of its location on the edge of the filter. The energy is split into an edge filter and an energy monitor channel that is used to normalize the edge filter signal. In a similar manner the laser energy backscattered from the atmosphere is collected with a telescope and is then measured with the edge detection setup to determine its frequency for each range element. The Doppler shift, and thus the wind, is determined from a differential measurement of the frequency of the outgoing

C. Flesia is with the Groupe de Physique Appliquée, Université de Genève, 20, rue de l'École de Médecine, 1211 Genève 04 Switzerland. Her email address is flesia@sc2a.unige.ch. C. L. Korb is with NASA Goddard Space Flight Center, Laboratory for Atmospheres, 912, Greenbelt, Maryland 20771. His email address is korb@agnes.gsfc.nasa.gov.

Received 20 January 1998; revised manuscript received 14 August 1998.

0003-6935/99/030432-09\$15.00/0

© 1999 Optical Society of America

laser pulse and the frequency of the laser return backscattered from the atmosphere. The differential frequency technique used to measure the Doppler shift renders the measurement insensitive to laser and filter frequency jitter and drift. A detailed description of the theory for the single-edge method is given in Ref. 1.

Korb *et al.* recently described a double-edge lidar technique for measuring the wind with the signal backscattered from aerosols in the atmosphere.¹⁶ With this method we use a second edge measurement for signal normalization rather than an energy monitor measurement, as is used in the single-edge technique. This technique doubles the sensitivity of an aerosol wind measurement relative to a single-edge aerosol wind measurement and yields an improvement in accuracy of nearly a factor of 2. In a similar manner we can use a double-edge technique for a molecular system to double the wind measurement sensitivity. We also describe a method for making the sensitivity of a wind measurement independent of whether the signal is backscattered from molecules or aerosols. We do this by locating the wind measurement in a region where the sensitivity of a molecular-based and an aerosol-based wind measurement are equal. This has the effect of desensitizing the molecular measurement to the effects of aerosol backscatter. The system we describe can use dual etalons for the edge filters, as is done in Chanin's system.^{8,9} However, unlike Chanin's system, ours is desensitized to the effects of aerosol scattering, uses a reference frequency measurement to control and correct for short- and long-term frequency errors, which is critical for a high accuracy wind measurement, and has greater sensitivity.

In the following sections we describe the theory of the double-edge measurement and the method of analysis, including methods for correcting frequency errors; measurement optimization; and methods of desensitizing the measurement to aerosol effects, the effects of R-B scattering, and simulation results.

2. Theory

Consider a laser located at frequency ν_l that is sent out and backscattered from molecules and aerosols in the atmosphere. The backscattered laser frequency is double Doppler shifted by the atmosphere by the amount of

$$\Delta\nu = \frac{2v}{c} \nu, \quad (1)$$

where v is the velocity of the wind along the line of sight of the laser beam, ν is the frequency of the laser, and c is the velocity of light. The backscattered laser signal as well as the outgoing laser signal is split between two edge filters as shown in Fig. 1. In addition, a few percent of the signal is directed to an energy monitor detector. The two edge filters centered at frequencies ν_1 and ν_2 are located in the wings of the R-B spectrum (see Fig. 2).

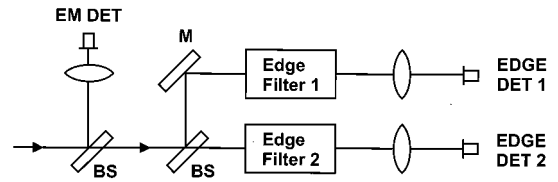


Fig. 1. Outgoing and backscattered laser signals split by a beam splitter (BS) and a mirror (M) between the two edge detector (EDGE DET) channels, and a small portion of the signal is sent to an energy monitor detector (EM DET).

The signal measured by edge filter one is

$$I_1 = a \left\{ \int_{-\infty}^{\infty} T_1(\nu - \nu_1) I_R[\nu - (\nu_l + \Delta\nu)] d\nu + I_A T_1(\nu_l + \Delta\nu - \nu_1) \right\}, \quad (2)$$

where a is a constant, I_R is the backscattered R-B spectrum, T_i is the transmission of the i th edge filter (T_i') for the laser, and I_A is the backscattered aerosol signal. In a similar manner, the signal measured by edge filter two is

$$I_2 = a \left\{ \int_{-\infty}^{\infty} T_2(\nu - \nu_2) I_R[\nu - (\nu_l + \Delta\nu)] d\nu + I_A T_2(\nu_l + \Delta\nu - \nu_2) \right\}. \quad (3)$$

When etalons are used as edge filters, T' is given by the Airy function, which is a Lorentzian for a single etalon fringe¹⁷; that is,

$$T_i'(\nu) = \frac{1}{1 + [(\nu - \nu_i)/\Delta\nu_i/2]^2}, \quad (4)$$

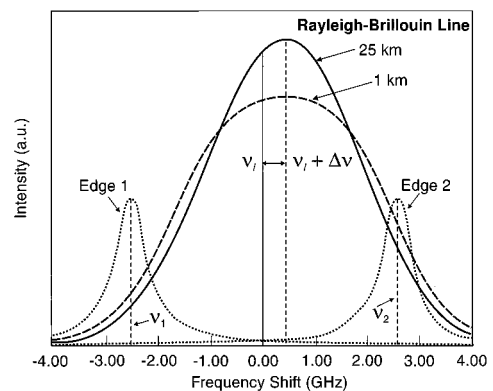


Fig. 2. Setup for the double-edge measurement of frequency shifts of the R-B profile with two edge filters at frequencies ν_1 and ν_2 .

where ν_i is the center frequency and $\Delta\nu_i$ is the full width at half-height (FWHH) of the i th filter. Let

$$R_1(\nu_1, \nu_l + \Delta\nu) = \int_{-\infty}^{\infty} T_1(\nu - \nu_1) I_R[\nu - (\nu_l + \Delta\nu)] d\nu, \quad (5)$$

$$R_2(\nu_2, \nu_l + \Delta\nu) = \int_{-\infty}^{\infty} T_2(\nu - \nu_2) I_R[\nu - (\nu_l + \Delta\nu)] d\nu; \quad (6)$$

then Eqs. (2) and (3) can be expressed as

$$I_1 = a[R_1(\nu_1, \nu_l + \Delta\nu) + I_A T_1(\nu_l + \Delta\nu - \nu_1)], \quad (7)$$

$$I_2 = a[R_2(\nu_2, \nu_l + \Delta\nu) + I_A T_2(\nu_l + \Delta\nu - \nu_2)]. \quad (8)$$

We can expand I_1 and I_2 about ν_l in a Taylor series as

$$I_1 = a \left\{ R_1(\nu_1, \nu_l) + I_A T_1(\nu_l - \nu_1) + \left[\frac{d}{d\nu} R_1(\nu_1, \nu_l) + I_A \frac{d}{d\nu} T_1(\nu_l - \nu_1) \right] \Delta\nu \right\}, \quad (9)$$

where

$$R_1(\nu_1, \nu_l) = R_1(\nu_1, \nu_l + \Delta\nu)|_{\Delta\nu=0},$$

$$\frac{d}{d\nu} R_1(\nu_1, \nu_l) = \left[\frac{d}{d\nu} R_1(\nu_1, \nu_l + \Delta\nu) \right]_{\Delta\nu=0},$$

and T_1 and its derivative are given in a manner similar to R_1 above. Equation (9) can be rewritten as

$$I_1 = a \left(R_1(\nu_1, \nu_l) + I_A T_1(\nu_l - \nu_1) + \Delta\nu \left\{ R_1(\nu_1, \nu_l) \times \left[\frac{1}{R_1(\nu_1, \nu_l)} \frac{d}{d\nu} R_1(\nu_1, \nu_l) \right] + I_A T_1(\nu_l - \nu_1) \times \left[\frac{1}{T_1(\nu_l - \nu_1)} \frac{d}{d\nu} T_1(\nu_l - \nu_1) \right] \right\} \right). \quad (10)$$

We can greatly simplify the analysis by locating the measurement in a crossover region such that

$$\frac{1}{R_1(\nu_1, \nu_l)} \frac{d}{d\nu} R_1(\nu_1, \nu_l) = \frac{1}{T_1(\nu_l - \nu_1)} \frac{d}{d\nu} T_1(\nu_l - \nu_1). \quad (11)$$

The use of this concept allows us to desensitize the molecular wind measurement to the effects of aerosol backscatter as discussed in Subsection 3.B.2. It then follows that

$$I_1 = a [R_1(\nu_1, \nu_l) + I_A T_1(\nu_l - \nu_1)] \times \left[1 + \frac{\Delta\nu}{R_1(\nu_1, \nu_l)} \frac{d}{d\nu} R_1(\nu_1, \nu_l) \right]. \quad (12)$$

This can be put in the form

$$I_1(\nu_1, \nu_l + \Delta\nu) = I_1(\nu_1, \nu_l) \left[1 + \frac{\Delta\nu}{R_1(\nu_1, \nu_l)} \frac{d}{d\nu} R_1(\nu_1, \nu_l) \right]. \quad (13)$$

In a similar manner,

$$I_2(\nu_2, \nu_l + \Delta\nu) = I_2(\nu_2, \nu_l) \left[1 + \frac{\Delta\nu}{R_2(\nu_2, \nu_l)} \frac{d}{d\nu} R_2(\nu_2, \nu_l) \right]. \quad (14)$$

If we define f as

$$f(\Delta\nu) = \frac{I_1(\nu_1, \nu_l + \Delta\nu)}{I_2(\nu_2, \nu_l + \Delta\nu)}, \quad (15)$$

it then follows from Eqs. (13)–(15) that

$$f(\Delta\nu) = f(0) \left\{ 1 + \left[\frac{1}{R_1(\nu_1, \nu_l)} \frac{d}{d\nu} R_1(\nu_1, \nu_l) - \frac{1}{R_2(\nu_2, \nu_l)} \frac{d}{d\nu} R_2(\nu_2, \nu_l) \right] \Delta\nu \right\} \quad (16)$$

to first order in $\Delta\nu$. This can be rewritten as

$$f(\Delta\nu) = f(0) [1 + (\vartheta_1' + \vartheta_2') \Delta\nu], \quad (17)$$

where

$$\vartheta_1' = \frac{1}{R_1(\nu_1, \nu_l)} \frac{d}{d\nu} R_1(\nu_1, \nu_l),$$

$$\vartheta_2' = \frac{-1}{R_2(\nu_2, \nu_l)} \frac{d}{d\nu} R_2(\nu_2, \nu_l) \quad (18)$$

are the sensitivities of the molecular measurement for a single edge,¹ taken in a positive sense, for a unit Doppler shift. It follows from Eq. (17) that the Doppler shift is given as

$$\Delta\nu = \frac{f(\Delta\nu) - f(0)}{f(0)(\vartheta_1' + \vartheta_2')} \quad (19)$$

and from Eqs. (1) and (19) that the wind velocity along the line of sight of the laser is

$$v = \frac{c}{2\nu} \frac{[f(\Delta\nu) - f(0)]/f(0)}{\vartheta_1' + \vartheta_2'}. \quad (20)$$

The measurement error along the line of sight is given in a manner similar to the double-edge aerosol experiment as¹⁶

$$\varepsilon = \frac{1}{(\vartheta_1 + \vartheta_2)(S/N)}, \quad (21)$$

where $\vartheta_1 + \vartheta_2$ is the sum of the sensitivities for the double-edge measurement for a unit velocity change

and S/N is the signal to noise for the ratio measurement of Eq. (15). The signal to noise is given as¹

$$\frac{1}{(S/N)} = \left[\frac{1}{(S/N)_1^2} + \frac{1}{(S/N)_2^2} \right]^{1/2}, \quad (22)$$

where $(S/N)_i$ is the signal to noise for the signal I_i .

3. Analysis

The double-edge molecular wind measurement is made in the region from 320 to 400 nm to take advantage of the high molecular backscatter, $\beta \propto \lambda^{-4}$, and to minimize absorption and scattering losses. A single-mode injection-seeded Nd:YAG laser is frequency tripled to provide narrow-band output at 355 nm with a width of the order of 200 MHz. This is nearly monochromatic with respect to the width of the R-B spectrum, 3.6 GHz FWHH, and easily meets the needs of the molecular measurement. For satellite-based measurements, Nd:YAG has the advantage that it can be diode pumped with relatively high efficiency and it has a long lifetime.

A. Correction of Frequency Error

The correction of frequency error is critical for a high accuracy wind measurement. There are two types of frequency error, short term and long term. The treatment of short-term error follows from Eq. (17), which gives the basic formulation of the double-edge molecular technique. The ratio of the Doppler-shifted signals backscattered from the atmosphere for the two edges $f(\Delta\nu)$ is given in terms of the ratio of the same backscattered atmospheric signals for zero Doppler shift $f(0)$ and the sum of the sensitivities for the two edges. The term $f(0)$ is given by Eq. (15) as

$$f(0) = I_1(\nu_1, \nu_l)/I_2(\nu_2, \nu_l). \quad (23)$$

We use the outgoing laser signal as measured by the edge filters as a reference to correct for laser or filter frequency jitter and drift. We note that the term $f(0)$ is not a measured quantity. We can find $f(0)$ as follows. First we determine the location of the laser on each edge filter by measuring the ratio of each edge signal to the energy monitor signal.¹ We then calculate the signals I_1 and I_2 as the convolutions of each edge filter with the laser and the R-B line profile and find $f(0)$ from Eq. (23). To calculate the R-B profile, we need an estimate of the temperature. We note that the width of the Rayleigh profile varies as the square root of the temperature. For zero Doppler shift and for a symmetric setup of the two etalons with respect to the laser, $f(0)$ is independent of temperature, because an increase in the width of the spectrum affects I_1 and I_2 equally (see Fig. 2). For a temperature of 250 K and with a 5K error in the temperature estimate, the resulting errors in the wind measurements that are due to the error in $f(0)$ are 0.11 and 0.55 m/s for wind velocities of 10 and 50 m/s, respectively.

Long-term frequency errors are removed with a servo control system, which is used to lock the edge of

each etalon fringe to the pulsed laser frequency. The measurement of the transmission of the outgoing laser signal on each edge filter is compared with a preselected value. A deviation from the preselected value is used to generate an error signal, which is used to tune the edge filter to compensate for the deviation. This system maintains each edge filter at approximately the correct location with respect to the laser frequency. High frequency accuracy is not required, because short-term frequency errors are removed with Eq. (23).

B. Measurement Optimization

1. General Factors

The backscattered signals from the atmosphere are split equally between the two-edge channels. A small percentage of the signal is split off and sent to an energy monitor channel, which is used for locking the edge filters to the laser frequency. That is, the transmission of the outgoing laser on each edge filter is determined from the ratio of the signal from each edge channel to the signal from the energy monitor channel.

We can optimize the performance of the measurement by minimizing the measurement error as given by Eq. (21). One of the key parameters that must be considered is the measurement sensitivity. We note that dividing by the sensitivity converts the fractional error in the measurement into an error in meters/second. Thus a doubling of the measurement sensitivity not only reduces the S/N required for a given error by a factor of 2, but it also reduces the effect of systematic errors by this same factor. This is of prime importance for a molecular measurement whereas the sensitivity is lower than for a corresponding aerosol-based edge measurement by a factor of approximately 10.

Figure 3 shows the measurement sensitivity of a molecular measurement as a function of the frequency separation between the laser and the Fabry-Perot etalons for various spectral resolutions. As shown, the measurement sensitivity generally increases as the spectral resolution increases. However, the higher the spectral resolution, the smaller the transmitted signal. Also, the peak of the curve moves further out on the R-B spectrum, which yields a lower signal and thus a lower S/N.

For a signal shot-noise-limited case, the S/N is proportional to the square root of the signal through the edge filter. We can define a figure of merit ϵ' for the measurement error as

$$\epsilon' = \frac{1}{(\vartheta_1 + \vartheta_2)\sqrt{R_1(V_1, V_l)}}.$$

Thus the smaller the value of ϵ' , the higher the performance.

Figure 4 gives ϵ' as a function of the location of the etalon on the R-B spectrum at an altitude of 10.1 km for various spectral resolutions. As shown, the error can vary by a factor of 2 as the separation of the laser and the edge filter varies from 1 to 3 GHz. The error

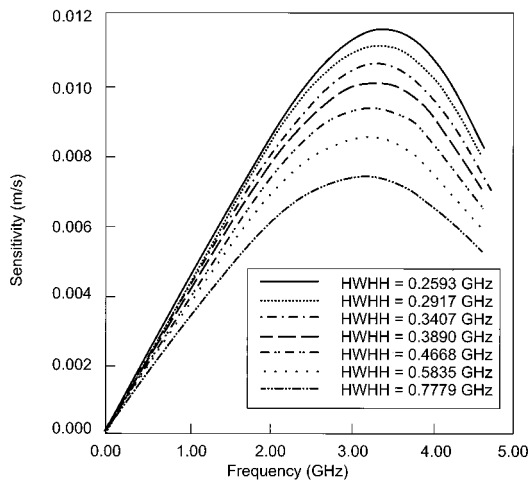


Fig. 3. Measurement sensitivity as a function of frequency for Fabry-Perot etalons for various spectral resolutions.

decreases slowly as the spectral resolution, half-width at half-height (HWHH), varies from 0.26 to 0.78 GHz.

The minimum error occurs for a Fabry-Perot etalon with a width of 0.778 GHz, HWHH, and the error has a relatively flat minimum for laser-edge filter separations from 2.1 to 2.6 GHz. As shown in Subsection 3.B.2, the measurement can be desensitized to the effects of aerosol scattering if the measurement is located at the crossover point, which corresponds to 3.31 half-widths, HWHH, for a Fabry-Perot etalon or a laser-edge filter separation of 2.58 GHz for an etalon with a half-width of 0.778 GHz, HWHH. It is important to note that the crossover location lies within 3% of the minimum error. Thus the molecular wind measurement can be desensitized to aerosol scattering effects while near optimum measurement error is achieved simultaneously.

2. Crossover Region

The edge filter measurement generally depends on the magnitude of the atmospheric backscattered mo-

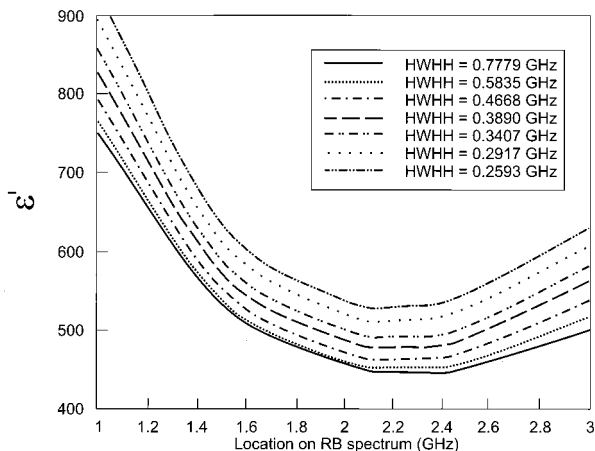


Fig. 4. Figure of merit for the measurement error for various spectral resolutions as a function of the location of the etalons on the R-B spectrum.

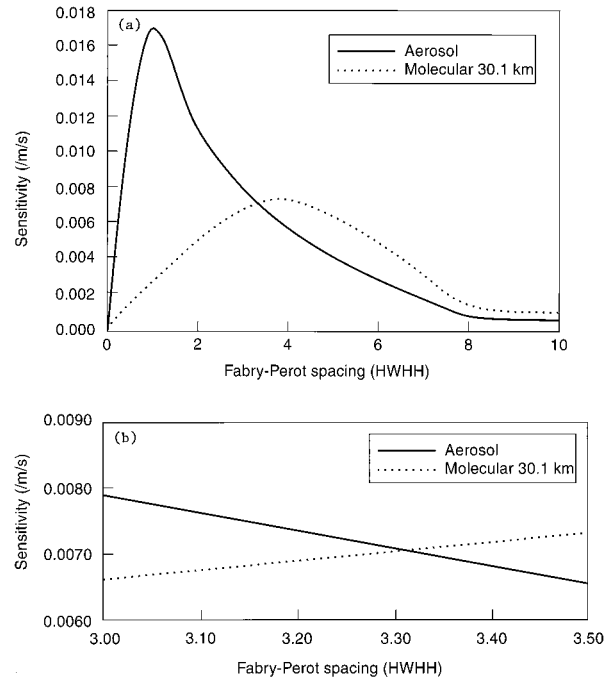


Fig. 5. Crossover region for the R-B profile at 30.1 km, which is close to a pure Rayleigh profile, for etalons used as edge filters for a spectral resolution, HWHH, of 0.778 GHz.

lecular, R-B, and aerosol signals [see Eqs. (2) and (3)]. Thus in general the molecular and aerosol signals have to be separated spectrally, measured separately, and treated independently in the analysis. We can, however, locate the edge filter measurement in a crossover region [see Eq. (11)] where the fractional change in the measured molecular and aerosol signals are equal for a given frequency shift. That is, the measurement sensitivities are equal for the molecular and aerosol portions of the signal. In this case the aerosol signal acts in a manner similar to the molecular signal, and the measurement is desensitized to the effects of aerosol scattering. This is one of the characteristics that separates the system we describe from that of Chanin,^{8,9} which does not use the crossover region.

Figure 5 shows the crossover region at a 30.1-km altitude, which is close to a pure Rayleigh line shape for the case of etalons used as edge filters with a spectral resolution of 0.778 GHz, HWHH. As shown, the sensitivity of the molecular- and aerosol-based measurements are equal at a distance of 3.31 etalon half-widths, HWHH, from the laser frequency. The sensitivity has a value of 0.72% m/s at the crossover point for the double-edge setup.

The double-edge system is balanced over a broad range of frequencies in the vicinity of the crossover frequency ν_c and not only at the particular crossover location if the edge filters are set up symmetrically about the laser frequency at the crossover location. Consider a Doppler shift $\Delta\nu$ about the crossover frequency ν_c . The Doppler-shifted spectrum has a mean frequency of $\nu_c + \Delta\nu$ for one edge filter and a frequency of $\nu_c - \Delta\nu$ for the second edge filter. The

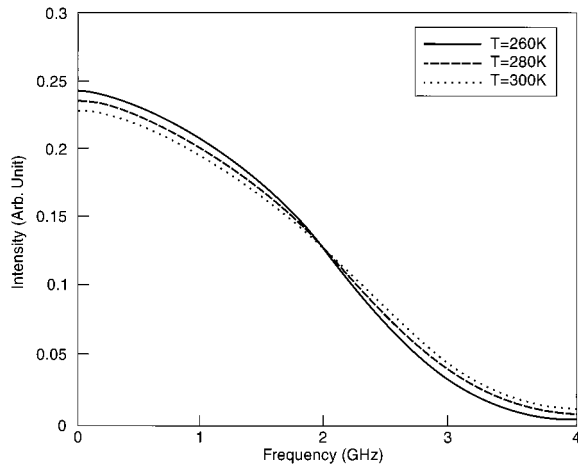


Fig. 6. R-B spectra at a wavelength of 355 nm at various temperatures for a pressure of 1000 mbars.

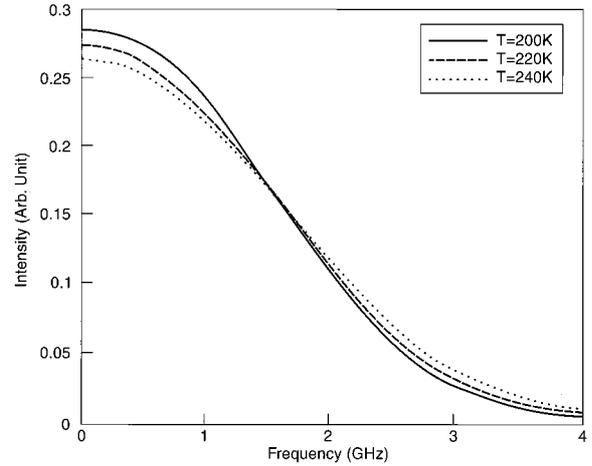


Fig. 8. R-B spectra at a wavelength of 355 nm at various temperatures for a pressure of 250 mbars.

effect of the Doppler shift on the molecular component of the spectrum is to produce a small increase in sensitivity for one edge filter and a small decrease in sensitivity for the other edge filter. The total sensitivity, $\vartheta_1' + \vartheta_2'$ [see Eq. (17)], tends to remain constant, i.e., balanced. If the sensitivity curve for the molecular spectrum had a linear variation in the vicinity of the crossover frequency, then the system would be perfectly balanced. The same discussion applies equally to the aerosol component of the spectrum; i.e., the aerosol component of the spectrum is also self-balancing. Thus the system is balanced over a range of frequencies for arbitrary molecular and aerosol backscatter levels. We note that the balancing imposes no constraints on the slopes of the molecular or aerosol sensitivity curves.

C. Rayleigh–Brillouin Scattering

Rayleigh scattering includes several scattering processes. R-B scattering results from fluctuations in the density of the media, and the Brillouin shift can be regarded as Doppler shifts that are due to the

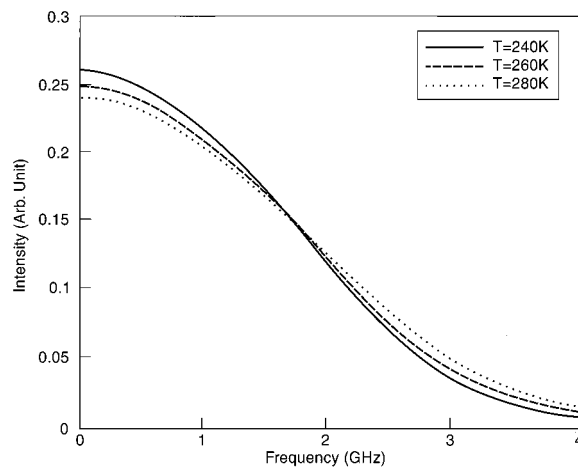


Fig. 7. R-B spectra at a wavelength of 355 nm at various temperatures for a pressure of 500 mbars.

moving fluctuations of sound waves. Brillouin scattering is inelastic, and with it new frequencies can arise. Thus the R-B spectrum can include both a central line that is due to light elastically scattered by density fluctuations in the gas, and two inelastically scattered Brillouin components that are symmetrically shifted about the central Rayleigh peak. The magnitude of the Brillouin shift is proportional to the speed of sound in the scattering medium and also depends strongly on the incident wavelength and scattering angle. As the gas density decreases, the R-B spectrum reduces to the familiar thermally broadened Rayleigh spectrum. In this regime, the individual molecules act as scatterers and the spectrum is Gaussian, which is produced by the Doppler shift of the individual molecules that move with an ensemble of velocities given by the Maxwell–Boltzmann velocity distribution.

In general the inelastic Brillouin scattered component must be included in the line profile in addition to the elastically scattered Rayleigh component. We modeled the R-B backscattered spectrum using the theory of Sugawara and Yip.¹² The R-B spectrum is a complex function of frequency, temperature, and pressure. Figures 6–8 show calculated spectra at a wavelength of 355 nm at various temperatures for pressures of 1000 mbars (Fig. 6), 500 mbars (Fig. 7), and 250 mbars (Fig. 8). As can be seen, the Brillouin peaks are not resolved and are barely apparent in the wings of the 1000-mbar spectra. As expected, the prominence of the Brillouin components decreases as the pressure decreases, and the features are not clearly evident in the 250-mbar spectra of Fig. 8. A high positive temperature sensitivity, i.e., a large positive fractional change in amplitude, is seen in the far wings of the spectra, whereas a relatively small negative temperature sensitivity is seen in the near wings of the spectra.

The sensitivity of the Doppler wind measurement technique, including the temperature and pressure sensitivity of the R-B spectrum, can be optimized. Figure 9 shows the calculated spectrum at a wave-

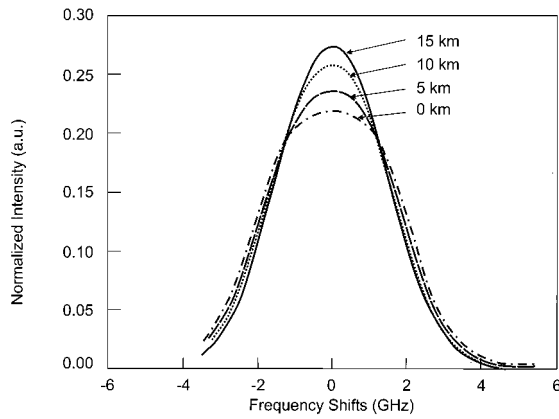


Fig. 9. R-B spectra at a wavelength of 355 nm for various altitude levels.

length of 355 nm for various altitude levels. As expected, the Brillouin component decreases with decreasing pressure. Two primary parameters of the high-resolution Fabry-Perot can be optimized, the etalon HWHH and the distance between the etalon fringe and the laser frequency. From previous results calculated at 30.1 km, which is close to a pure elastic Rayleigh line shape, the laser is located at 3.31 HWHH from the center of each etalon fringe for an etalon HWHH of 0.778 GHz. This value is the crossover point at which the sensitivity, the percentage change in signal for a 1-m/s wind, is equal for both Rayleigh and aerosol signals.

For the same value of the etalon width, calculations with the R-B spectrum show, as expected, an altitude dependence of the crossover point (see Fig. 10). The crossover point varies between 3.31 half-widths, HWHH, at a 30.1-km altitude, and 3.40 half-widths, HWHH, at a 1-km altitude, which corresponds to a change in the etalon sensitivity from 0.72 to 0.74%/m/s, respectively. If we optimize the system for a 5-km altitude, then the etalons are located symmetrically about the laser at 3.35 etalon half-widths, a separation of 5.21 GHz. Our discussion above of the

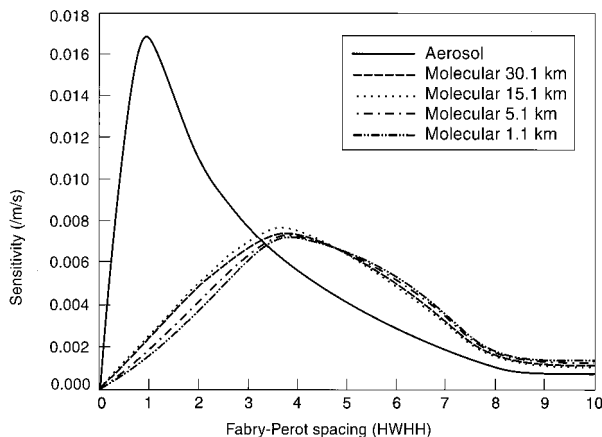


Fig. 10. Altitude dependence of the crossover region for the R-B profile for etalons used as edge filters with a spectral resolution of 1.56 GHz.

Table 1. Satellite Lidar System Simulation Parameters

Platform measurement characteristics	
Altitude (km)	400
Scan pattern	45° Conical
Spatial resolution (km × km)	200 × 200
Vertical resolution (km)	1
Shots averaged	72
Laser	
Wavelength (nm)	355
Energy (J)	1
Spectral width (MHz)	200
Receiver	
Telescope diameter (m)	0.9
Field of view (mrad)	0.1
Optical efficiency ^a	0.46
Beam splitter	48/48
Transmission/reflectance	
Detector	PMT
Quantum efficiency (%)	25
Etalon	
Spacing (cm)	1.25
Free spectral range (GHz)	12
Spectral width (FWHM, GHz)	1.56
Effective finesse	7.71
Etalon separation (GHz)	5.21

^aThe optical efficiency does not include the beam splitter transmission/reflectance or the etalon transmission.

balancing properties of the crossover region also applies to the R-B profile. We note that the maximum variation in the sensitivity at the extreme altitudes is $\pm 0.01\%$ m/s about the mean value, which corresponds to a maximum wind error of 1.4% (as a percentage of the wind value if this effect were not accounted for).

D. Simulations

To evaluate the performance, we present the results of simulations for a satellite-based system. The parameters for the satellite system are as follows. The satellite altitude is 400 km. We used a 45° conical scan with photomultiplier tube (PMT) detectors, which gives a swath width of 800 km. This produced a spatially representative measurement. The parameters for the satellite-based system are shown in Table 1. We considered wind measurements with a spatial resolution of 200 km × 200 km and a 1-km vertical resolution. The time to traverse 200 km along the spacecraft velocity vector is 28.6 s for a satellite velocity of 7 km/s. This yields an average measurement time of 7.2 s for each 200 km × 200 km spatial element. For a 20-Hz laser repetition rate, there are 144 shots per spatial element, assuming the shots are uniformly distributed over each spatial element. To determine the two horizontal components of the velocity, two different viewing directions are used for each spatial element. Thus there are 72 shots for measurements in both the forward and backward viewing directions. We used a Nd:YAG single longitudinal mode laser operating at 20 Hz with an output energy of 3 J/pulse at 1064 nm, a pulse length of 8 ns,

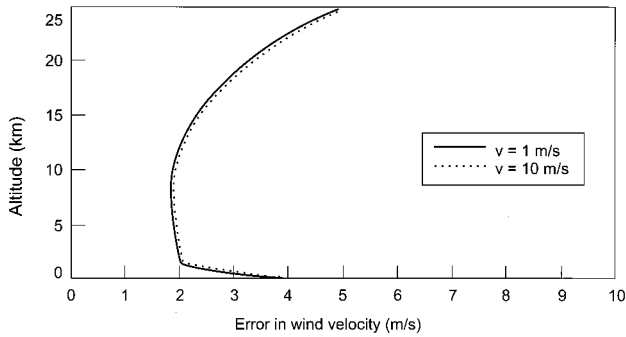


Fig. 11. Simulation results for a satellite-based 355-nm double-edge system at 400 km for a 1-J laser energy, a 200 km \times 200 km spatial resolution, and a 1-km vertical resolution.

and a linewidth of 80 MHz. The laser output energy is frequency tripled to 355 nm, which yields 1 J/pulse with a linewidth of 200 MHz.

Our atmospheric model uses the 1985 U.S. Standard Atmosphere for the molecular backscatter and the globe north median distribution for the aerosol model.¹¹ We use the Airy function to represent the etalons, which have a spectral width, FWHH, of 1.56 GHz and a separation from the laser of 2.605 GHz. The model of Sugawara and Yip¹² is used for R-B scattering. We use a single-scattering model for these simulations, because clouds are not included in these simulations and the contribution of multiple scattering is negligible. We included the effects of 600 dark counts/s that are due to the PMT detector and the effects of a daylight background (20% albedo), but the effect was small, because we used narrow-band interference and etalon background blocking filters. We assumed the reference frequency measurement was made with the outgoing laser pulse with a much higher S/N than the atmospheric return pulse and thus introduced negligible error.¹ The errors are given for measurements along the line of sight of the laser beam. The simulation results for the satellite-based system are shown in Fig. 11. As shown, the error in the wind velocity varies from 2 to 3 m/s over the altitude range from 2 to 15 km for wind velocities that vary from 0 to ± 100 m/s.

4. Conclusion

A double-edge lidar technique for measuring the wind with molecular backscatter has been described. The technique uses two high-spectral-resolution edge filters that are located in the wings of the R-B profile. It has been shown that this doubles the signal change for a given Doppler shift, the sensitivity of the measurement, which leads to improvement in measurement accuracy by a factor of nearly 2. We have described the theory and use of a crossover region, the point at which the sensitivity of a molecular- and an aerosol-based wind measurement is equal. If the edge filters are located at this point, then the aerosol signal acts in the same manner as the molecular signal. This has the effect of desensitizing the mo-

lecular measurement to the effects of aerosol backscatter. We also have shown that measurements at the crossover location lie within 3% of the minimum error. The use of double-edge filters allows the system to be balanced not only at the crossover location but also over a range of frequencies with a width of the order of ± 100 m/s.

We have given methods for optimizing the performance of the measurement and have shown that edge filters with a spectral width, FWHH, of 1.56 GHz at 355 nm produce measurement sensitivities of 0.73% m/s at the crossover location. We have described a method for correcting for short-term frequency jitter in the etalon or laser with a laser reference frequency measurement. We have also described a method of removing long-term frequency drifts using the reference measurement to lock the etalons to the laser frequency with a servo control system. We have shown that the effects of R-B scattering on the measurement are significant and have included these effects in our analysis. The results of simulations for a conically scanned satellite system at 400-km altitude show that an accuracy of 2–3 m/s can be obtained over the altitude range of 2–15 km for a 1-km vertical resolution, a 200 km \times 200 km spatial resolution, a 0.9-m-diameter telescope, and a laser energy of 1 J/pulse.

This research was supported by the Swiss National Science Foundation, NASA under contract RTOP 460-28-45, and the U.S. Army Research Office under contract AR096-25.

References

1. C. L. Korb, B. Gentry, and C. Weng, "The edge technique: theory and application to the lidar measurement of atmospheric winds," *Appl. Opt.* **31**, 4202–4213 (1992).
2. B. Gentry and C. L. Korb, "Edge technique for high-accuracy Doppler velocimetry," *Appl. Opt.* **33**, 5770–5777 (1994).
3. C. L. Korb, B. Gentry, and S. X. Li, "Edge technique Doppler lidar wind measurements with high vertical resolution," *Appl. Opt.* **36**, 5976–5983 (1997).
4. V. J. Abreu, "Wind measurements from an orbital platform using a lidar system with incoherent detection: an analysis," *Appl. Opt.* **18**, 2992–2997 (1979).
5. V. J. Abreu, J. E. Barnes, and P. B. Hays, "Observations of winds with an incoherent lidar detector," *Appl. Opt.* **31**, 4509–4514 (1992).
6. M. J. McGill, W. R. Skinner, and T. D. Irgang, "Analysis techniques for the recovery of winds and backscatter coefficients from a multiple-channel incoherent Doppler lidar," *Appl. Opt.* **36**, 1253–1268 (1997).
7. D. Rees and I. S. McDerimid, "Doppler lidar atmospheric wind sensor: reevaluation of a 355-nm incoherent Doppler lidar," *Appl. Opt.* **29**, 4133–4144 (1990).
8. M. L. Chanin, A. Garnier, A. Hauchecorne, and J. Porteneuve, "A Doppler lidar for measuring winds in the middle atmosphere," *Geophys. Res. Lett.* **16**, 1273–1276 (1989).
9. A. Garnier and M. L. Chanin, "Description of a Doppler Rayleigh LIDAR for measuring winds in the middle atmosphere," *Appl. Phys. B* **55**, 35–40 (1992).
10. W. R. Skinner and P. B. Hays, "A comparative study of coherent and incoherent Doppler lidar techniques," Rep. NAS8-38775, (Marshall Space Flight Center, Huntsville, Ala., 1994).

11. J. D. Spinhirne, S. Chudamani, J. F. Cavanaugh, and J. L. Bufton, "Aerosol and cloud backscatter at 1.06, 1.54, and 0.53 μm by airborne hard-target-calibrated Nd:YAG/methane Raman lidar," *Appl. Opt.* **36**, 3475–3490 (1997).
12. A. Sugawara and S. Yip, "Kinetic model analysis of light scattering by molecular gases," *Phys. Fluids* **18**, 1911–1921 (1967).
13. G. Tenti, C. D. Boley, and R. D. Desai, "On the kinetic model description of Rayleigh–Brillouin scattering from molecular gases," *Can. J. Phys.* **52**, 285–290 (1974).
14. G. Tenti and R. D. Desai, "Kinetic theory of molecular gases I/models of the linear Waldmann–Snider collision operator," *Can. J. Phys.* **53**, 1266–1278 (1974).
15. C. D. Boley, R. D. Desai, and G. Tenti, "Kinetic models and Brillouin scattering in a molecular gas," *Can. J. Phys.* **50**, 2158–2173 (1972).
16. C. L. Korb, B. M. Gentry, S. X. Li, and C. Flesia, "Theory of the double-edge technique for Doppler lidar wind measurement," *Appl. Opt.* **37**, 3097–3104 (1998).
17. F. Bayer-Helms, "Analyse von Linienprofilen. I. Grundlagen und Messeinrichtungen," *Z. Agnew. Phys.* **15**, 330–338 (1963).